REPRESENTATIVE PEDESTRIAN COLLISION INJURY RISK DISTRIBUTIONS FOR A DENSE-URBAN US ODD USING NATURALISTIC DASH CAMERA DATA

Eamon T. Campolettano
John M. Scanlon
Trent Victor
Waymo, LLC
United States

Paper Number 23-0075

ABSTRACT

Automated Driving Systems (ADS; SAE levels 3 through 5 technologies) are currently being deployed in several dense-urban operational design domains (ODDs) within the United States (US). Within these dense-urban areas, vulnerable road users (VRU) generally comprise the vast majority of injury and fatal collisions. One challenge with the study of VRU collisions is a lack of crash data sources with pre-impact kinematics. Understanding the pre-impact kinematics is a key factor in assessing the potential injury risk for pedestrian-vehicle impacts. The purpose of this study was to determine injury distributions for pedestrians within a dense-urban ODD (Los Angeles, California) using data from vehicles instrumented with forward-facing cameras and vehicle sensors. This study leveraged data from a fleet of vehicles equipped with aftermarket, in-cabin dash cameras operating in Los Angeles, California. From approximately 66 million miles of driving data, 42 collisions were identified. Each vehicle was equipped with a forward-facing camera, an accelerometer sampling at 20 Hz, and GPS. A global optimization routine was used on the accelerometer, GPS, and video data to correct for sensor orientation and asynchronicity in data sampling. For each event, two key video frames were identified: the frame associated with impact and a frame associated with key vehicle kinematics (e.g., vehicle start/stop, hard braking [> 0.2 g]). These key frames were then mapped to the processed vehicle speed kinematics to determine vehicle speed at impact.

For the events included in this dataset, impact speeds ranged from approximately 1.6 kph (1 mph) to 65 kph (40 mph). In most events, the front of the vehicle struck the pedestrian. Existing pedestrian injury risk curves were then used to calculate the level of risk associated with the reconstructed impacts, and the probability of AIS3+ injury risk was observed to vary from minimal risk (<2%) to approximately 55%. These data highlight the wide range of impact speeds and injury risk that may occur during vehicle-pedestrian collisions.

Assessing injury severity for collisions involving VRUs is highly impactful for the continued development of traffic safety, including ADAS, ADS, and roadway design. Using naturalistic VRU collision data collected from dashboard cameras, a methodology for assessing event severity by pairing accelerometer and GPS data with video to compute impact speed was presented. This is the first known analysis of pedestrian severity distributions using a naturalistic US database. The methods presented in this study may be applied to larger datasets or other sensing systems to enable further ODD-specific modeling.

INTRODUCTION

Pedestrians represent a vulnerable group of road users who do not have the same crash protections as vehicle occupants during a collision event. According to the most recent data available from NHTSA, over 6,000 pedestrians were fatally injured in 2019, compared to over 75,000 who sustained injuries in traffic-related crashes [1]. Furthermore, pedestrians represent 17% of all police-reported traffic collision-related fatalities, but only 3% of all such injuries [1]. In general, fatal pedestrian collisions were most likely to occur in urban areas (82%), at non-intersections (73%), and 90% of all fatal collisions occurred due to contact with the front of the vehicle [1].

The majority of pedestrian impact events in human collision data occur with the front structures of some forward moving vehicle [1-4]. Accordingly, injury risk models are often built using this frontal striking data. During these events, some pedestrian actor is within the trajectory of some vehicle actor when the engagement occurs. Injuries generally occur following some engagement of the front bumper structure. This is followed by potential movement of the pedestrian onto the hood, windshield, A-pillar, and other structures. Lastly, there can be potential ground contact. Injuries can occur during any phase of this engagement. Because of these injury-causing mechanisms, the

previously developed models overwhelmingly utilize vehicle impact speed as a key independent variable dictating injury risk [5-10].

Analysis from an in-depth, German collision database called German In-Depth Accident Study (GIDAS) has shown that approximately 88% of collisions involving pedestrians resulted in a maximum injury severity of MAIS2 or lower [11]. Regardless of severity, the lower extremity is the most often-injured body region (injured in 67% of cases), followed by the head (~50% of the time), and upper extremity (38% of the time). The lower extremity is most often injured by contact with the front end of the striking vehicle, while the most common injury source for the head is engagement with the windshield, followed by the ground [12-14].

From 1994 to 1998, the National Traffic Highway Safety Administration (NHTSA) oversaw the Pedestrian Crash Data Study (PCDS). PCDS compiled data from crashes involving pedestrians in 6 geographic areas and resulted in in-depth analysis on 549 total collision events [15]. To date, PCDS represents the most comprehensive large-scale pedestrian crash database in the United States with objective injury outcome data; however, the data is not recent, not of a representative sample, and only considers frontal impacts and not all pedestrian-vehicle events. When relating injury risk to vehicle impact speed, Tefft noted that the age of PCDS may affect the relationship due to "changes in medical care, vehicle design, or the composition of the vehicle fleet [10]."

Previously, researchers have utilized taxicabs instrumented with forward-facing cameras and vehicle sensors in South Korea to investigate injury severity for collisions involving pedestrians. Notably, injury severity was only presented on an ordinal scale based on data from police reports rather than utilizing an existing probabilistic injury risk model. As in previous research, crash speed was highly related to injury severity [16].

ADS fleets are currently being deployed in several dense-urban US operational design domains (ODDs). For example, Waymo has commercial ride-hailing operations in downtown Phoenix and the Phoenix East Valley [17], and has been testing without an autonomous specialist behind the wheel in San Francisco since early 2022 [18]. Within these dense-urban areas, vulnerable road users (VRU), such as pedestrians, generally comprise the vast majority of injury and fatal collisions [1, 3-4]. One challenge with the study of VRU collisions is a lack of crash data sources with objective pre-impact kinematics. Understanding the pre-impact kinematics is a key factor in assessing the potential injury risk for pedestrian-vehicle impacts. The purpose of the present study was to determine injury risk distributions for pedestrians within a dense-urban ODD (Los Angeles, California) using data from vehicles instrumented with forward-facing cameras and vehicle sensors in conjunction with established pedestrian injury risk models.

METHODOLOGY

Data Source

This study leveraged data from a fleet of vehicles equipped with aftermarket in-cabin dash cameras operating in Los Angeles, California. For this study, only collision events and driving miles on S1400 roads were included. S1400 roads are defined as "local neighborhood road, rural road, city street [19]." From approximately 66 million miles of driving data, 42 collisions involving pedestrians were identified and considered in this study.

Each vehicle was equipped with a forward-facing camera, an accelerometer sampling at 20 Hz, and GPS.

Video Review

Video of each collision was reviewed and agreed upon by two of the authors to determine several, mostly qualitative factors associated with the collision event. Specifically, the nature of the vehicle engagement with the pedestrian (frontal strike, sideswipe, side collision, rear strike), the location on the vehicle of the initial contact (e.g., front left, right front, rear), the relative direction of engagement between the pedestrian and vehicle (i.e., perpendicular vs. parallel), whether the pedestrian engaged with side structures of the vehicle, how many pedestrians were involved in the collision event, and whether the pedestrian was knocked down were all evaluated. These data were utilized as part of the ensuing analysis leveraging the on-board sensor data.

Vehicle Impact Speed Determination

To make an injury risk assessment, vehicle impact speed measurements were required (a key input to the injury risk function evaluation). A vehicle speed measurement was provided via the GPS sensor. However, the GPS speed had

inconsistent sampling and limited resolution. Accordingly, the GPS speed was coupled with accelerometer data. Accelerometer data was available for all cases with either a low pass filter at 0.5 Hz or 5 Hz applied to the data. The traces filtered at 5 Hz were used for this analysis considering collision events because the jerk associated with vehicle hard braking was captured with this signal and not smoothed as part of the filtering process like it was for the 0.5 Hz data. A series of steps were required to (a) correct for inconsistent sensor orientation within the vehicle and (b) align the speed and accelerometer data due to asynchronous data collection. These steps to generate a single, corrected vehicle speed are covered in the subsequent subsections.

Sensor Orientation Correction The installed dash cams used in this study were found to have considerable variability in their orientation within the vehicle. Specifically, although the dash camera unit was oriented largely in the forward direction, there was some notable pitch as evidenced by non-zero acceleration z-direction (upwards and downwards; after correcting for acceleration due to gravity) while the equipped vehicle was stopped. To correct for this pitch, a correction routine was applied. This routine assumed that the true signal for longitudinal vehicle acceleration ($acc_{x,\,corrected}$) was measured in part by the longitudinal and vertical accelerometer data as shown in Equation 1, where θ corresponds to the angular pitch offset of the sensor with respect to the z-direction being up and down.

$$acc_{x,\,corrected} = acc_x cos(\theta) + acc_z sin(\theta) \qquad \text{Equation (1)}$$

Further, any periods of time during which the vehicle was not accelerating (i.e., constant travel speed or a stopped vehicle) the x-component as measured by the accelerometer should be approximately equal to 0 as well. By integrating over these time periods (where both the change in velocity in the x and z directions should be zero; equation 2), an estimate of the sensor pitch (θ) can be determined (Equation 3).

$$0 = \int acc_x cos(\theta) dt + \int acc_z sin(\theta) dt \qquad \text{Equation (2)}$$

$$tan(\theta) = -\frac{dv_x}{dv_z} \qquad \text{Equation (3)}$$

With the sensor pitch defined, the longitudinal vehicle acceleration could be calculated using the x and z accelerometer signals.

Speed and Acceleration Optimization Given the lower sampling rate for the speed data from the GPS, the accelerometer data were leveraged, through integration, to generate a higher sampling rate speed vector. The accelerometer and GPS data were collected asynchronously from one another, which prevented straightforward integration. A global optimization routine was used to perform a temporal correction on these data to align the GPS speed and accelerometer data for each case. An iterative routine was carried out that applied a temporal shift to the accelerometer data prior to integrating to generate velocity values. These velocity values were then compared to those provided by the GPS data, and the difference between the integrated accelerometer speed and the GPS speed represented integration drift, or the error in the velocity signal. The time shift that minimized the velocity error was selected as the optimal outcome and was saved for continued data analysis.

The accelerometer data were used to calculate what the expected velocity would be based on the mean acceleration between two time points and the preceding known velocity. At the unique velocities extracted from the GPS data, the error between the measured and expected velocities was calculated. Lastly, as shown in Equation 4, the corrected vehicle speed ($v_{corrected,\,i}$) was calculated at successive time points using the expected speed for that time point ($v_{expected,\,i}$) in conjunction with a time-scaled version of the calculated velocity error ($Error_j$). To account for noise associated with small velocity values, all velocity values below 0.5 mph were set to 0 mph.

$$v_{corrected,\,i} = v_{expected,\,i} + Error_j * \frac{t_i - t_{j-1}}{t_j - t_{j-1}} \qquad \text{Equation (4)}$$

where i is as defined above and represents indexing over the entire length of the velocity trace and j represents indexing over the vector of unique velocity values. Thus, at all times when $t_i = t_j$, no time-scaling was necessary and the corrected velocity reduces to the sum of the expected velocity and the error term. This method also ensures that the corrected speed was equal to the GPS speed at each of the unique velocity value timepoints previously identified. This optimization process was repeated for each time shift evaluated (increments of 0.05 s), and the temporal shift which resulted in the minimum mean absolute velocity error was selected as the optimized version to carry forward in analysis. An example of the results of the optimization process is shown in Figure 1.

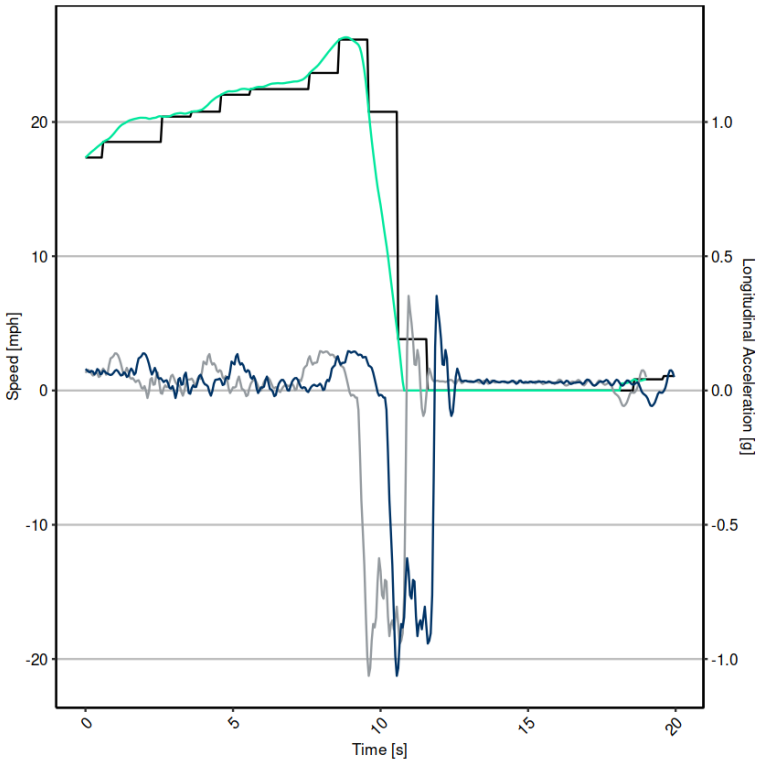

Figure 1. Exemplar sensor optimization trace. Gray line represents original longitudinal vehicle acceleration, dark blue line represents time-shifted longitudinal vehicle acceleration, black line represents GPS speed, and green line represents the corrected vehicle velocity trace.

Impact Speed Determination The final step in determining vehicle impact speed was to align the video with the imputed vehicle speed. Key, easily identifiable kinematic time points from the video were associated to kinematic signatures from the vehicle speed time series. Depending on the specific collision, different alignment routines were applied. In all collisions, two video frames were identified: the frame associated with vehicle impact and a frame associated with key vehicle kinematics (e.g., vehicle start/stop, hard braking [> 0.2 g]; see Table 1). These key frames were then mapped to the processed vehicle speed kinematics outlined above to determine vehicle speed at impact. Given the video frame rate (4 Hz), the exact time of impact was generally not captured. Accordingly, the nearest frame preceding collision was used. The speed at the time point closest to this time was taken to be the vehicle impact speed. All collision videos were sampled at 4 frames per second and were 20 or 30 seconds in length. Individual frames were extracted from downloaded collision videos using ffmpeg (ffmpeg.org).

Table 1.
Vehicle kinematics used for key frame for determination of vehicle speed at impact and description of how specific frame was defined

Vehicle Kinematics	**Description**
Vehicle stop	Vehicle stop was determined based on video-observed braking to a stop. With the available vehicle speed data collected by the accelerometers, the time point at which the vehicle's speed first achieved a value of 0 mph was found. The nth stop was used, with the time associated with the beginning of each stop found using the accelerometer data.
Minimum/maximum speed	When a kinematic visual cue was not available, the vehicle's minimum or maximum speed was used as a reference point. This method required an iterative process involving simultaneous review of the accelerometer data and collision video. The time point in the accelerometer data associated with either the highest or lowest vehicle speed was found.
Start from first stop	The vehicle was at rest prior to accelerating and then involved in a collision. The frame associated with vehicle motion following this stop was used in conjunction with the impact frame. The accelerometer data was first used to find the time at which the vehicle first comes to rest. Then, the first time point following that at which the vehicle was moving is determined to be the time associated with the start from first stop.
Hard braking (> 0.2 g)	There was a defined spike in the vehicle's accelerometer pulse associated with deceleration that occurred either prior to or after the collision. The time point in the accelerometer data associated with vehicle braking exceeding 0.2 g was found.
Vehicle in reverse	Visual confirmation of impact was not possible given that the available video footage was for the forward-facing camera only. For this situation, the frame at which the vehicle began to reverse and the frame in which the vehicle came to rest were identified. In these instances, the maximum speed observed in the accelerometer data during this time window (i.e., the time of reversal) was taken to be the estimate for vehicle impact speed.
Last frame	The collision occurred near the end of the video and no specific vehicle kinematics could be ascertained (e.g., vehicle did not come to rest before end of video). The number of video frames between collision and the end of the video were used to determine the time of impact, and thus the vehicle's speed at impact.

While most collision events were frontal impacts, some involved engagement with side vehicle structures instead of the front bumper structure. To account for decreased engagement between the pedestrian and vehicle during these side impacts, a correction factor - representing a decrease in the impulse experienced by the pedestrian - was applied to the determined impact speed for these collisions based on previous work. This correction factor was based on Neale et al.'s photogrammetric analysis of video recordings of pedestrian sideswipe and minor overlap impact events [20]. In their work, vehicle speed at impact was computed for each event and compared to the predicted vehicle impact speed based on measured pedestrian projection distance. Level of engagement with the vehicle was found to vary depending on the nature of the collision and was lower than would be expected in a frontal collision [21]. Correction factors to the vehicle impact speed for these projection models were presented to account for the decreased impulse experienced by the pedestrian during the collision event. For this study, a scaling factor of 1.5 was applied for collisions involving side contact to account for this decrease in engagement (i.e., a side collision at 15 mph would be modeled as if it were a 10 mph frontal collision).

Injury Severity Assessment

This study relied on previously published injury risk curves by Lubbe et al. to translate the computed impact speed to a probability of injury based on severity of injury as defined by the 2015 revision of the Abbreviated Injury Scale (AIS) [22]. The AIS is an internationally recognized scale that scores injuries, considering "energy dissipation, tissue damage, treatment, impairment, and quality of life [22]." Lubbe et al. developed an injury risk function relating vehicle closing speed and pedestrian age to AIS2+, AIS3+, and fatal injury outcomes for frontal collisions involving pedestrians based on data from the German In-Depth Accident Study (GIDAS) [23]. The dataset used to develop the injury risk functions only consisted of collisions involving passenger vehicles; accordingly, vehicle mass/weight for the vehicles included in the SmartDrive dataset as part of this study was not considered. Lubbe et al.'s study considered pedestrians aged 15 and older. An average risk curve was fit using logistic regression based on the weighted distribution of pedestrians age 15+ in the Crash Report Sampling System (CRSS) to simplify evaluation of injury risk to only be dependent on speed. It should be noted that pedestrian speed was not considered as part of this analysis as it was assumed that the pedestrian's motion would not be expected to contribute substantially to the injury risk. Accordingly, vehicle speed at impact (v) was used for injury risk assessment instead of closing speed. These relationships are summarized in Equations 5, 6, and 7.

$$p(AIS2+) = 1/(1 + e^{1.824-0.060*v}) \quad \text{Equation (5)}$$

$$p(AIS3+) = 1/(1 + e^{4.257-0.073*v}) \quad \text{Equation (6)}$$

$$p(Fatal) = 1/(1 + e^{7.000-0.087*v}) \quad \text{Equation (7)}$$

RESULTS

In general, most collisions in this dataset (34 out of 42) involved frontal vehicle structures (Figure 2). This is consistent with previous research of field crash data, which has shown that the frontal collision mode is the most common and most injurious [23]. The overall crash rate for this dataset was 0.63 collisions per million miles.

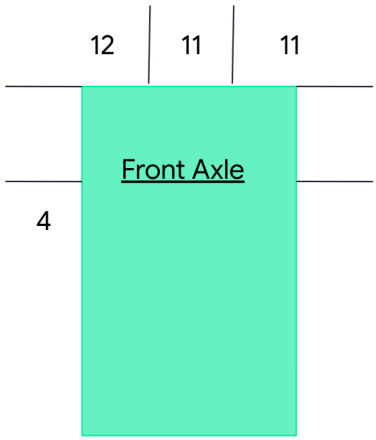

Figure 2. Distribution of collision counts by impact location on vehicle

Vehicle impact speeds into the pedestrians varied from 1.5 mph to 38 mph. More than half of all events had an impact speed less than 10 mph and nearly all (38 out of 42) events had an impact speed less than 20 mph (Figures 3 and 4).The pedestrian collision events were associated with a wide range of MAIS2+ injury risk probabilities, from as low as 12% up to 85%. The majority of events were associated with an MAIS3+ injury risk probability below 10%, with only 5 events exceeding 10% and 2 exceeding 50% MAIS3+ injury risk (Figure 3). Almost all events were associated with a very low probability of fatal injury (Figure 4). Summed MAIS2+, MAIS3+, and fatal injury risk for this dataset totaled approximately 14, 3, and 0.5, respectively. In other words, given objective injury

outcome data for the pedestrians involved in these collisions, it would be expected that approximately 14 would sustain MAIS2+ injuries, approximately 3 would sustain MAIS3+ injuries, and approximately 0.5 would sustain fatal injuries. These expected injury outcomes may also be calculated as a measure of mileage in order to more accurately compare across datasets. For this dataset, we would expect to see a moderate or greater injury (MAIS2+) every 4.6 million miles, a serious or greater injury (MAIS3+) every 20 million miles, and a fatal injury (MAIS5+) every 128 million miles.

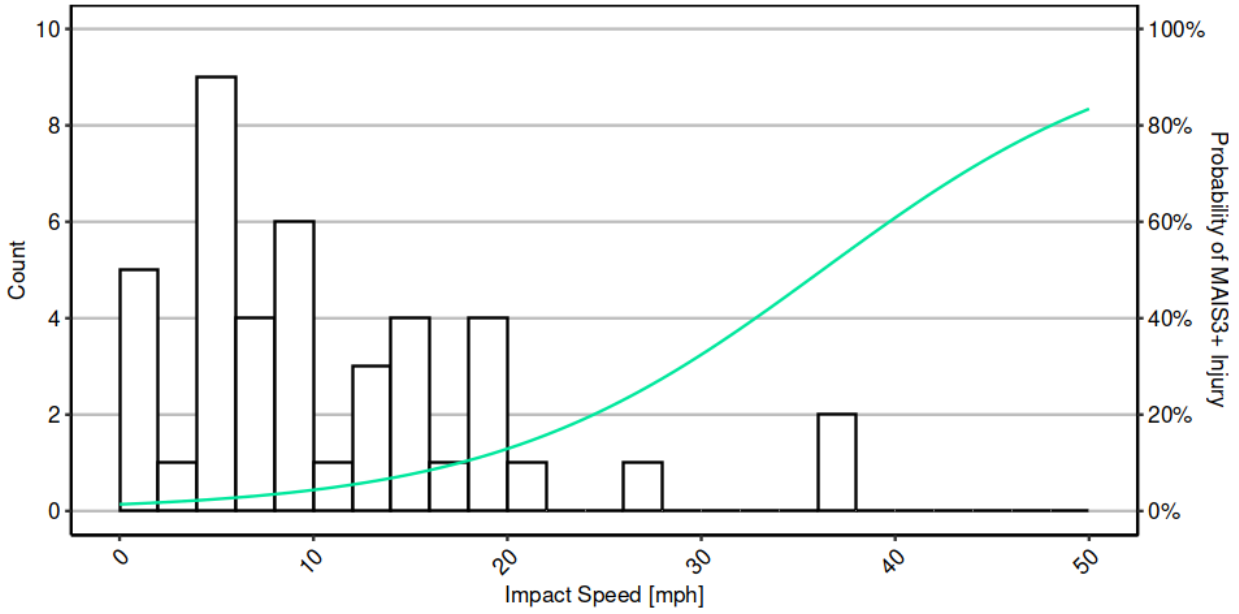

Figure 3. Distribution of events and MAIS3+ injury risk as a function of impact speed. Nearly all events were associated with an impact speed of less than 20 mph.

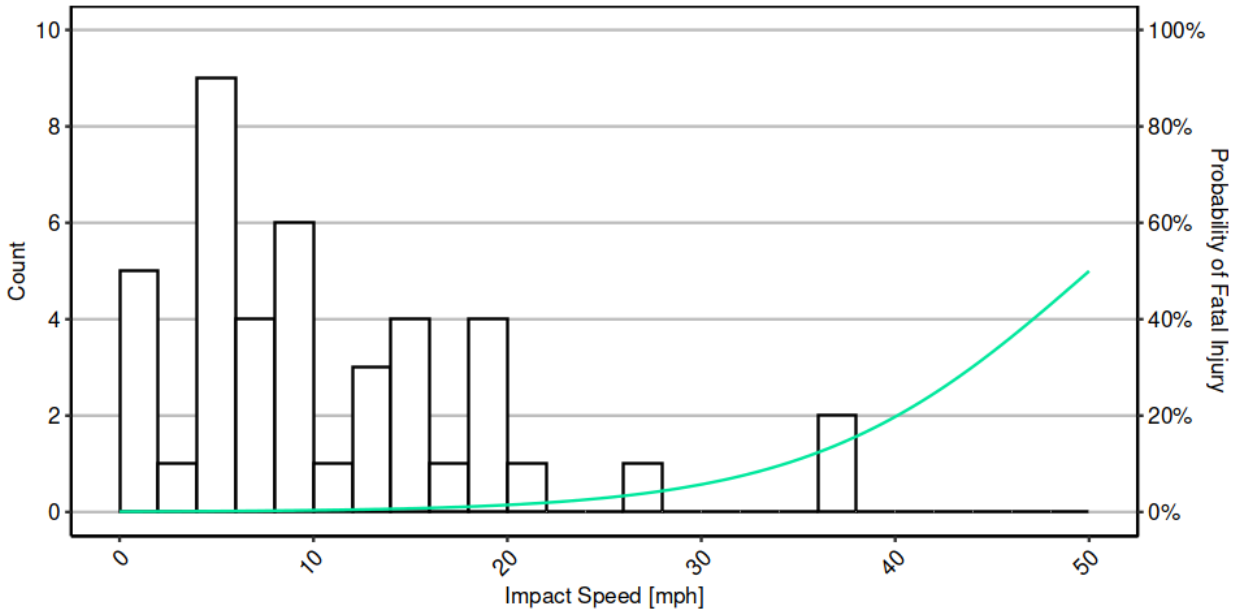

Figure 4. Distribution of events and fatal injury risk as a function of impact speed. Nearly all events were associated with a fatal injury risk probability near zero.

Impact speed was also observed to vary by vehicle turning behavior. Many of the collision events in this representative dataset occurred at an intersection, and of those events, left and right turning was frequently observed.

A wide range of vehicle impact speeds was observed for situations in which the vehicle was traveling straight prior to the collision (Figure 5). In general, the act of turning prior to the collision led to lower traveling speeds, and accordingly, generally lower impact speeds. Additionally, narrower speed windows were observed when the vehicle was turning. Specifically, impact speeds associated with the vehicle making a right turn were all below 10 mph, while impact speeds associated with the vehicle making a left turn ranged from below 10 mph to over 20 mph (Figure 5).

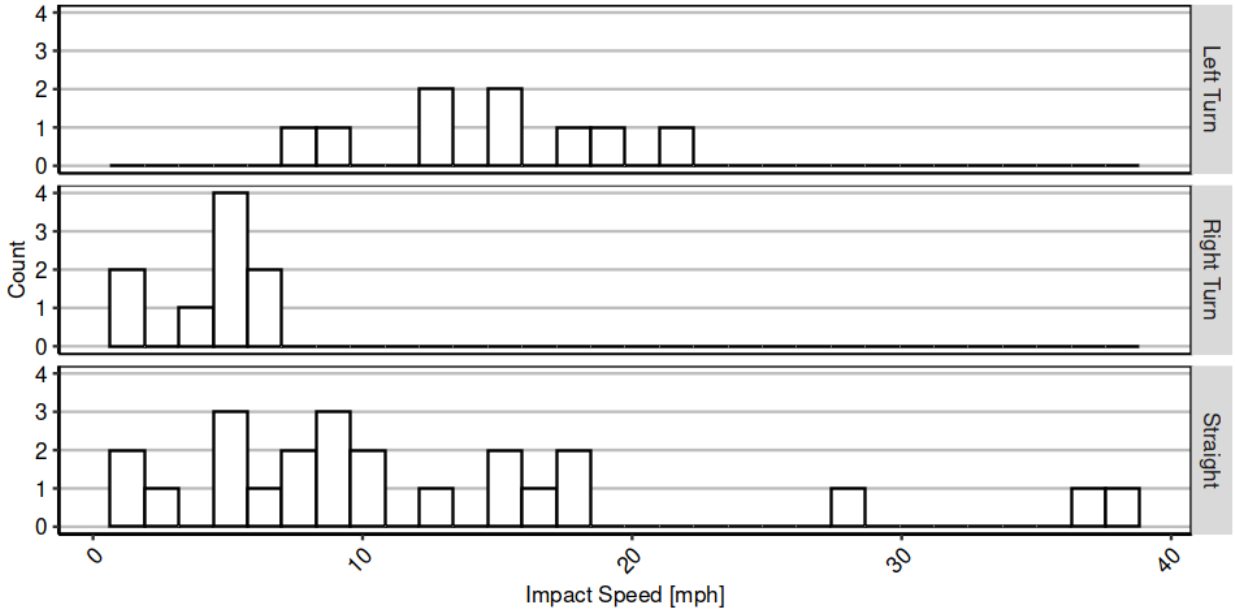

Figure 5. Distribution of events as a function of impact speed by vehicle travel behavior at the time of collision.

Pedestrian knock-down risk was also explored. Using the available collision video, only collisions with known impact speeds and knock pedestrian knock-down status were included as part of this analysis (i.e., cases where the video cut off or the pedestrian was out of frame after the collision event were excluded). Leveraging the assigned knock-over status based on review of the collision videos, a logistic regression model was developed to estimate risk of pedestrian knock-over as a function of collision speed. A 10% risk of knockdown was observed to occur at 2.8 mph (Figure 6). It should also be noted that in collisions with impact speeds above 10 mph, all pedestrians were knocked over.

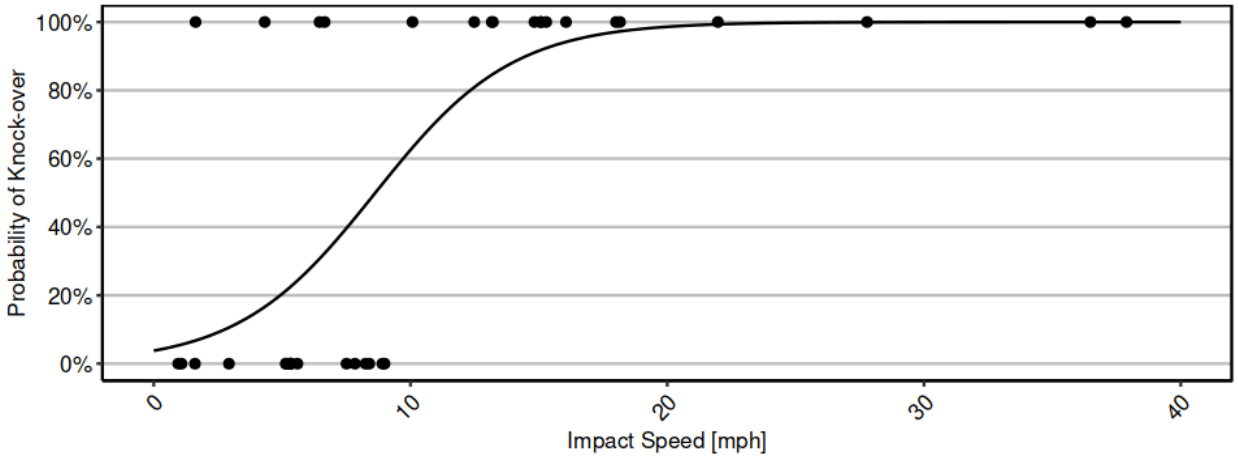

Figure 6. Pedestrian knock-over risk as a function of impact speed. Events were evaluated binarily, as knock-over (1, 100%) or no knock-over (0, 0%).

DISCUSSION

Using the dash cam video and sensor data, impact speed was successfully extracted for all 42 pedestrian impact events considered in this study. Nearly all the events involved collision with the front portion of the vehicle, which enabled the impact to be readily identified and associated to the imputed vehicle speed. The outcome of this analysis is a representative dataset of collisions with corresponding injury from surface streets in Los Angeles, California.

In general, the number of injured persons in collisions may be lowered through reduction in the number of collisions, reduction in the severity of the collisions, and/or reduction in the injury risk associated with a given collision severity [24]. The present study offers insight into the severity of existing collisions and the predicted injury risk associated with them. One challenge in evaluating ADS technology is that retrospective safety benefits using in-field driving are typically established using historical crash outcomes, where a decrease in injury outcomes is used as evidence of safety impact [25-29]. Injuries, however, are relatively rare, which makes any statistical assertions using high severity outcomes alone require an extreme number of miles (e.g., billions of miles to prove a reduction in fatal injury outcomes) [30-31].

Injury outcomes are rare, but the conditions for creating those outcomes are considerably more frequent. Scanlon et al. (2021 and 2022) showed it was not uncommon for serious or greater (MAIS3+) injury risk to be below 25% in reconstructed cases where a fatality was observed [32-33]. This is illustrative of the probabilistic nature of injuries, where the conditions for injuries to occur are more common than the occurrence of the injury itself. Looking at the current study, although it comprises only 66 million miles worth of driving, several events had serious or greater (MAIS3+) injury risk over 10%. As an alternative to measuring serious injury, or worse, outcomes, measuring the frequency of the high severity potential conditions can be used as an early signal when evaluating safety benefits. For example, ISO 26262 uses the “S” severity grading scale using 10% risk of various AIS level probabilities (MAIS 1+, 3+, 5+) to bucket events according to injury risk in functional safety applications [34]. Relying on this probabilistic injury risk, rather than the occurrence of the injury, should theoretically provide earlier evidence of what safety impact is being achieved. These individual event injury risk predictions may be additionally leveraged by summing across all events to determine some measure of the overall expected injury outcome rate. Using this approach, the cumulative injury risk is being assessed, where one event with 50% probability of injury is treated equally as five events with a 10% probability of injury. This has previously been done in the field of automotive safety and sports head impact research [35-41] Scanlon 2017, Scanlon 2016]. As stated above, for the pedestrians involved in the collisions in this dataset, it would be expected that approximately 3 would sustain serious or greater injury (MAIS3+) injuries or that a similar injury would be expected to occur every 20 million miles of driving. These mileage-adjusted injury rates would be the metrics of interest when comparing human driving data with simulated or real collision data for autonomous vehicles in order to determine relative driving performance or in comparing across different ODDs.

Overall, the impact speeds were observed to follow a multimodal distribution (Figure 3). Controlling for turning behavior substantially limited outcome severity magnitude and variability, which clearly indicates the influence of turning on collision impact speed and, accordingly, injury risk. In most cases where vehicles were making right turns from a stop and did not accelerate to speed prior to engaging with a pedestrian; conversely, vehicles making left turns often engaged with the pedestrian when they were nearly complete with the left turn, after having traveled a greater distance and thus having a greater opportunity to achieve higher vehicle speed at impact. These observations are consistent with vehicle-to-vehicle intersection collisions in the United States, where impact speeds are dependent on turning behavior and stopping behavior [35, 39, 42-43]. Turning while traveling through intersections (without coming to a complete or rolling stop) notably features a general slowing prior to the turn with a generally constant speed during travel through the intersection.

For this dataset, there was a larger proportion of events associated with impact speeds between 5 and 10 mph than between 0 and 5 mph. This sort of distribution is also observed in intersection cross-traffic, where a severity risk “cliff” exists at the borderline of a small overlap strike and a near-miss (an analogous example of this risk cliff would be stepping in front of a moving train). It is also believed that low severity impacts are more easily avoidable by pedestrians. Although not explicitly examined in the current study, postural changes and evasive action were found to limit engagement between the pedestrian and vehicle at lower speeds. Several cases in this dataset included

instances of pedestrian adjustment to avoid or mitigate energy transfer during the collision, which was commonly observed as a rapid juke away from the approaching vehicle sometimes with outstretched arms that engaged the forward structures of the vehicle. This sort of complexity when developing injury risk curves is not commonly captured in the absence of first hand video footage. Additionally, these events are subject to underreporting given that the maneuvering can serve to prevent and mitigate a potential injury. Previous research reviewing video of pedestrian-to-vehicle collision events has shown that nearly two-thirds of pedestrians take avoidance action prior to the collision event [44]. This observed pedestrian avoidance action clearly plays a role in the level of engagement and potential injury risk for pedestrian collisions. Incorporation of this feature into the severity evaluation of observed collisions should be explored.

Review of the collision videos highlighted the effect of factors such as pedestrian age and pre-impact posture as also likely playing a role in pedestrian knock-down. At these lower speeds in which the pedestrians were knocked down, injury would primarily be expected to occur due to falling from standing height to the ground rather than from engaging with vehicle structures. An in-depth review of 100 pedestrian-to-vehicle collision in Paris, France showed that contact with the ground was the source of injury for over a quarter of all impacts with impact speeds less than 31 mph (50 kph) and more than half of all impacts with speeds below 18.6 mph (30 kph) [4].

Limitations

There are several limitations of this work that should be noted. Firstly, there were differences in sampling frequency for the GPS, accelerometers, and camera such that the original data were not synchronized. Corrections and temporal shifts were applied to the data to minimize error in computed impact speeds as part of the collision reconstruction. Secondly, pedestrian speed was not considered as part of this analysis; however, nearly all impacts involved a perpendicular collision between a vehicle and a pedestrian, and the pedestrian's motion would not be expected to contribute substantially to the injury risk.

There are also some notable limitations with the utilized injury risk model that may influence the accuracy of any individual risk estimation. First, only frontal collisions are considered. Use of this function for side impacts and rear collisions may result in some unquantified deviation from actual risk. Second, this data was developed using German crash data from 1999 to 2020. Differences in the composition of this fleet with respect to the current United States fleet may lead to some unquantified accuracy deviations. Third, for a case to be included in the dataset, the pedestrian must be suspected of having experienced some injury. It is common for police-reported pedestrian data to almost always have an associated pedestrian injury, so this data requirement is unsurprising. Still, collisions without an injury are not considered, resulting in data censoring and low-end risk offsets.

CONCLUSIONS

Assessing injury severity for collisions involving VRUs is highly impactful for the continued development of traffic safety, including ADAS, ADS, and roadway design. Using naturalistic VRU collision data collected from dashboard cameras, a methodology for assessing event severity by pairing accelerometer and GPS data with video to compute impact speed was presented. This is the first known analysis of pedestrian severity distributions using a naturalistic US database. The methods presented in this study may be applied to larger datasets or other sensing systems to enable further ODD-specific modeling of the current crash population.

REFERENCES

[1] National Center for Statistics and Analysis. (2021). Pedestrians: 2019 data (Traffic Safety Facts. Report No. DOT HS 813 079). National Highway Traffic Safety Administration.
[2] Martin, J. L., & Wu, D. (2018). Pedestrian fatality and impact speed squared: Cloglog modeling from French national data. *Traffic injury prevention*, 19(1), 94-101.
[3] European Commission (2021) Road safety thematic report – Pedestrians. European Road Safety Observatory. Brussels, European Commission, Directorate General for Transport.
[4] Guillaume, A., Hermitte, T., Hervé, V., & Fricheteau, R. (2015). Car or ground: which causes more pedestrian injuries. In *24th International Technical Conference Enhanced Safety Vehicle*.
[5] Davis, G. A. (2001). Relating severity of pedestrian injury to impact speed in vehicle-pedestrian crashes: Simple threshold model. *Transportation research record*, 1773(1), 108-113.

[6] Niebuhr, T., Junge, M., & Achmus, S. (2013). Pedestrian injury risk functions based on contour lines of equal injury severity using real world pedestrian/passenger-car accident data. *Annals of advances in automotive medicine*, 57, 145.
[7] Richards, D. C. (2010). Relationship between speed and risk of fatal injury: pedestrians and car occupants. Department for Transport: London.
[8] Rosén, E., & Sander, U. (2009). Pedestrian fatality risk as a function of car impact speed. *Accident analysis & prevention*, 41(3), 536-542.
[9] Saadé, J., Cuny, S., Labrousse, M., Song, E., Chauvel, C., & Chrétien, P. (2020). Pedestrian injuries and vehicles-related risk factors in car-to-pedestrian frontal collisions. In *Proceedings of the 2020 IRCOBI Conference* (pp. 278-289). Munich: IRCOBI.
[10] Tefft, B. C. (2011). Impact speed and a pedestrian's risk of severe injury or death. AAA Foundation for Traffic Safety.
[11] Otte, D., Jänsch, M., & Haasper, C. (2012). Injury protection and accident causation parameters for vulnerable road users based on German In-Depth Accident Study GIDAS. *Accident analysis & prevention*, 44(1), 149-153.
[12] Badea-Romero, A., & Lenard, J. (2013). Source of head injury for pedestrians and pedal cyclists: Striking vehicle or road?. *Accident analysis & prevention*, 50, 1140-1150.
[13] Fredriksson, R., Rosén, E., & Kullgren, A. (2010). Priorities of pedestrian protection—a real-life study of severe injuries and car sources. *Accident analysis & prevention*, 42(6), 1672-1681.
[14] Mallory, A., Fredriksson, R., Rosén, E., & Donnelly, B. (2012). Pedestrian injuries by source: serious and disabling injuries in US and European cases. In *Annals of Advances in Automotive Medicine/Annual Scientific Conference* (Vol. 56, p. 13).
[15] Chidester, A. B., & Isenberg, R. A. (2001). The pedestrian crash data study. In *Proceedings: International Technical Conference on the Enhanced Safety of Vehicles* (Vol. 2001, pp. 12-p). National Highway Traffic Safety Administration.
[16] Chung, Y. (2018). Injury severity analysis in taxi-pedestrian crashes: An application of reconstructed crash data using a vehicle black box. *Accident analysis & prevention*, 111, 345-353.
[17] *Phoenix*. Waymo. Retrieved December 5, 2022, from https://waymo.com/phx/
[18] *Waypoint - the official waymo blog: Taking our next step in the city by the Bay*. Waypoint – The official Waymo blog. (2022, March 30). Retrieved December 5, 2022, from https://blog.waymo.com/2022/03/taking-our-next-step-in-city-by-bay.html
[19] US Census Bureau. (2010). 2010 TIGER/Line® Shapefiles Technical Documentation.
[20] Neale, W. T., Danaher, D., Donaldson, A., & Smith, T. (2021). Pedestrian Impact Analysis of Side-Swipe and Minor Overlap Conditions. *SAE Technical Paper*, 01-0881.
[21] Toor, A., & Araszewski, M. (2003). Theoretical vs. empirical solutions for vehicle/pedestrian collisions. *SAE transactions*, 853-865.
[22] Association for the Advancement of Automotive Medicine. (2016). The Abbreviated Injury Scale: 2015 Revision. Chicago, IL: AAAM.
[23] Lubbe, N., Wu, Y., & Jeppsson, H. (2022). Safe speeds: fatality and injury risks of pedestrians, cyclists, motorcyclists, and car drivers impacting the front of another passenger car as a function of closing speed and age. *Traffic Safety Research*, *2*.
[24] Kullgren, A. (2008). Dose-response models and EDR data for assessment of injury risk and effectiveness of safety systems. In *Proc of Int. IRCOBI Conf., Bern, Switzerland* (pp. 3-14).
[25] Blower, D., & Woodrooffe, J. (2013). *Real-World Safety Effect of Roll Stability Control* (No. 2013-01-2392). SAE Technical Paper.
[26] Cicchino, J. B. (2017). Effectiveness of forward collision warning and autonomous emergency braking systems in reducing front-to-rear crash rates. *Accident analysis & prevention*, 99, 142-152.
[27] Isaksson-Hellman, I., & Lindman, M. (2015). Real-world performance of city safety based on Swedish insurance data. In *24th international technical conference on the enhanced safety of vehicles (ESV)* (Vol. 8, pp. 15-0121).
[28] Partnership for Analytics Research in Traffic Safety (2022). *Real-world Effectiveness of Model Year 2015–2020 Advanced Driver Assistance Systems*. The MITRE Corporation.
[29] Riexinger, L., Sherony, R., & Gabler, H. (2019). *Has Electronic Stability Control Reduced Rollover Crashes?* (No.2019-01-1022). SAE Technical Paper.
[30] Kalra, N., & Paddock, S. M. (2016). Driving to safety: How many miles of driving would it take to demonstrate autonomous vehicle reliability?. *Transportation Research Part A: Policy and Practice*, 94, 182-193.

[31] Lindman, M., Isaksson-Hellman, I., & Strandroth, J. (2017). Basic numbers needed to understand the traffic safety effect of automated cars. In *Proceedings of the 2017 IRCOBI Conference* (pp. 1-12).
[32] Scanlon, J. M., Kusano, K. D., Daniel, T., Alderson, C., Ogle, A., & Victor, T. (2021). Waymo simulated driving behavior in reconstructed fatal crashes within an autonomous vehicle operating domain. *Accident Analysis & Prevention*, 163, 106454.
[33] Scanlon J. M., Kusano, K. D., Engstrom, J., & Victor, T. (2022). Collision Avoidance Effectiveness of an Automated Driving System Using a Human Driver Behavior Reference Model in Reconstructed Fatal Collisions.
[34] International Organization for Standardization. (2018). 26262-3: 2018. Road vehicles—Functional safety—Part 3: Concept phase.
[35] Bareiss, M., Scanlon, J., Sherony, R., & Gabler, H. C. (2019). Crash and injury prevention estimates for intersection driver assistance systems in left turn across path/opposite direction crashes in the United States. *Traffic injury prevention*, 20(sup1), S133-S138.
[36] Campolettano, E. T., Gellner, R. A., Sproule, D. W., Begonia, M. T., & Rowson, S. (2020). Quantifying youth football helmet performance: assessing linear and rotational head acceleration. *Annals of biomedical engineering*, *48*(6), 1640-1650.
[37] Kusano, K. D., & Gabler, H. C. (2012). Safety benefits of forward collision warning, brake assist, and autonomous braking systems in rear-end collisions. *IEEE Transactions on Intelligent Transportation Systems*, *13*(4), 1546-1555.
[38] Scanlon, J. M., Kusano, K. D., & Gabler, H. C. (2016). Lane departure warning and prevention systems in the US vehicle fleet: Influence of roadway characteristics on potential safety benefits. *Transportation Research Record*, *2559*(1), 17-23.
[39] Scanlon, J. M., Sherony, R., & Gabler, H. C. (2017). Injury mitigation estimates for an intersection driver assistance system in straight crossing path crashes in the United States. *Traffic injury prevention*, 18(sup1), S9-S17.
[40] Stemper, B. D., Shah, A. S., Harezlak, J., Rowson, S., Mihalik, J. P., Duma, S. M., et al. (2019). Comparison of head impact exposure between concussed football athletes and matched controls: evidence for a possible second mechanism of sport-related concussion. *Annals of biomedical engineering*, *47*(10), 2057-2072.
[41] Urban, J. E., Davenport, E. M., Golman, A. J., Maldjian, J. A., Whitlow, C. T., Powers, A. K., & Stitzel, J. D. (2013). Head impact exposure in youth football: high school ages 14 to 18 years and cumulative impact analysis. *Annals of biomedical engineering*, *41*(12), 2474-2487.
[42] Scanlon, J. M., Sherony, R., & Gabler, H. C. (2017). Models of driver acceleration behavior prior to real-world intersection crashes. *IEEE Transactions on intelligent transportation systems*, 19(3), 774-786.
[43] Scanlon, J. M. (2017). *Evaluating the Potential of an Intersection Driver Assistance System to Prevent US Intersection Crashes* (Doctoral dissertation, Virginia Tech).
[44] Han, Y., Li, Q., He, W., Wan, F., Wang, B., & Mizuno, K. (2017). Analysis of vulnerable road user kinematics before/during/after vehicle collisions based on video records. In *IRCOBI Conference, Antwerp, Belgium* (pp. 13-15).